Progress of Theoretical Physics, Vol. 113, No. 4, April 2005

The Higgs Sector in the Next-to-MSSM

Koichi FUNAKUBO[1,*] and Shuichiro TAO[2,**]

[1]*Department of Physics, Saga University, Saga 840-8502, Japan*
[2]*Department of Physics, Kyushu University, Fukuoka 812-8581, Japan*

(Received October 1, 2004)

We study the Higgs sector in the next-to-minimal supersymmetric standard model both with and without explicit CP violation, focusing on the case of a weak-scale expectation value of the singlet field. We scan a wide range of the parameter space to determine allowed regions by requiring that the electroweak vacuum be the global minimum of the effective potential and that the neutral Higgs bosons with moderate gauge coupling be heavier than the lower bound on the Higgs boson in the standard model. Among the allowed sets of parameter values, some sets yield the situation in which the light Higgs bosons couple with the Z boson too weakly for observation to be possible in present collider experiments. For such parameter sets, we determine an upper bound on the charged Higgs mass that is attainable in LHC.

§1. Introduction

The search for the Higgs boson is one of the most important issue of high-energy particle physics, because the Higgs boson is the only unobserved particle in the minimal standard model (MSM). The results of the LEP 2 experiment place a limit on the MSM-Higgs mass: $m_h > 114.4$ GeV with 95% CL.[1),2)] Although there are some theoretical restrictions on the Higgs mass, it cannot be predicted in the MSM framework, because the Higgs self-coupling is a free parameter. Supersymmetric extensions of the MSM, which were formulated with the goal of solving the hierarchy problem, place limitations on the possible range of the Higgs mass, because of the self-coupling resulting from the gauge couplings. Among such extensions, the minimal supersymmetric Standard Model (MSSM) has been extensively studied and is known to give an upper bound on the mass of the lightest Higgs boson, namely, $m_h \leq m_Z$ at the tree level. This bound seems somewhat severe, but it is modified by radiative corrections, through which it becomes $m_h \leq 135$ GeV at the two-loop level. These corrections come mainly from the loops of the top quark and squark.[3)]

The MSSM contains a μ-parameter in the superpotential. It enters the Higgs potential with the soft scalar masses to determine the vacuum expectation value (VEV) of the Higgs fields. Thus, μ must take a value on the order of the weak scale, which is much smaller than the GUT scale or Planck scale. However, there is no *a priori* reason for μ to have such a small value. One solution of this so-called μ-problem is to substitute a VEV of an extra gauge-singlet field for the parameter μ. The NMSSM is among the models that have a gauge-singlet Higgs superfield N.

*) E-mail: funakubo@cc.saga-u.ac.jp
**) E-mail: tao@higgs.phys.kyushu-u.ac.jp

The superpotential of the model contains

$$W = -\lambda N H_d H_u - \frac{1}{3}\kappa N^3, \tag{1·1}$$

in addition to the MSSM terms with $\mu = 0$.[4] We adopt the Z_3-symmetric version of the superpotential so that it does not contain any dimensional coupling. The μ-parameter of the MSSM is generated as $\mu = \lambda \langle N \rangle$. The NMSSM behaves like the MSSM in the limit that $\langle N \rangle \gg v$ with $\lambda\langle N \rangle$ and $\kappa\langle N \rangle$ fixed, in which case the singlet decouples. Here $v = \sqrt{\langle H_d \rangle^2 + \langle H_u \rangle^2}$ is the VEV of the Higgs doublets. Because the superpotential has no dimensional parameters, the VEVs of the Higgs fields are determined by the mass parameters in the soft-supersymmetry-breaking terms together with the couplings. If all the mass parameters in the Higgs potential are of the weak scale and all the couplings have moderate values approximately in the range 0.1 – 1, it is natural for the singlet to acquire a VEV of the same order as v. Then we expect there to appear features that do not exist in the MSSM, and our main concern is the Higgs sector in this case.

The NMSSM contains three CP-even neutral Higgs bosons, S_1, S_2 and S_3, two CP-odd bosons, A_1 and A_2, and a pair of charged bosons, $H^\pm$, in the CP-conserving case. The spectrum of the CP-conserving model is studied in Refs. 5)–7). In contrast to the situation in the MSSM, in the NMSSM the three CP-even scalars can mix to form mass eigenstates of small mass with very small gauge coupling.[7] Such a light Higgs boson cannot be produced in lepton colliders, and therefore it is not excluded, even if its mass is smaller than 114 GeV. We refer to this situation as the *light Higgs* scenario. As we see below, such a light Higgs situation is realized in the case of weak scale $\langle N \rangle$ and small κ. A similar situation has been observed in the MSSM when a large mixing among CP eigenstates is caused by the CP violation in the squark sector, which is characterized by the imaginary part of the product of μ and the A-term.[8] Then the gauge coupling of the lightest scalar is so small that it can escape the lower bound on the Higgs mass.[9] While the same mixing is also expected in the NMSSM, it contains another source of CP violation in the tree-level Higgs sector. Such a CP violation has been studied in several cases in which it is caused spontaneously[10] and explicitly[11] in some special situations. We give the one-loop formulation with all possible CP phases including the squark sector in a manner that is independent of the phase convention. In this formulation, one can easily arrange the phases in such a way that the phase relevant to the neutron electric dipole moment (nEDM) is suppressed while those which affect the mixing of the Higgs bosons are retained. We investigated the mass spectrum and couplings in the case that such a CP phase is included.

Another aspect of the NMSSM Higgs sector is that the Higgs potential contains cubic terms including the singlet field. Although these terms must be constrained in such a manner that they do not cause the global minimum of the effective potential to differ from the electroweak vacuum, they are expected to strengthen the first-order phase transition at high temperature. In this sense, this model is more suited for electroweak baryogenesis than is the MSSM, which requires a light stop with a mass less than the top quark mass for the strongly first-order phase transition.[12]

We pointed out that the CP violation in the squark sector weakens the electroweak phase transition (EWPT) caused by a light stop in the MSSM.[13] We conjecture that, in contrast to the MSSM, the CP violation in the Higgs sector of the NMSSM does not weaken the EWPT, while being sufficient to generate chiral charge flux, which is the source of baryon asymmetry. The effects of this CP violation on the phase transition will be discussed in a forthcoming paper.

This paper is organized as follows. In §2, we analyze the NMSSM Higgs sector at the tree level and explain how to obtain restrictions on the parameters in the model. There we derive the upper and lower bounds on the mass of the charged Higgs, which are trivial in the MSSM limit but important in the case of weak scale $\langle N \rangle$. In §3, we derive the one-loop formulas for the mass-squared matrix of the neutral Higgs bosons and the mass of the charged Higgs boson. In §4, we present the results of the numerical parameter search. The spectrum condition divides the allowed parameter sets into two classes. The first class consists of MSSM-like allowed parameter sets, in which all the Higgs bosons are heavier than 114 GeV, and the second class corresponds to the light Higgs scenario. The study of the CP violation is described in §5. The formulas used to define the effective potential and to calculate the mass matrix are summarized in the appendices.

§2. Tree-level Higgs sector

2.1. *Higgs potential*

In this section we analyze the tree-level Higgs sector. The NMSSM has the following superpotential with the singlet superfield N:[7]

$$W = f_d H_d Q D^c - f_u H_u Q U^c - \lambda N H_d H_u - \frac{\kappa}{3} N^3. \tag{2·1}$$

Here Q, D^c and U^c denote chiral superfields containing quarks, and H_d and H_u contain the Higgs doublets required in the MSSM. The couplings λ and κ for the singlet are in general complex numbers. We consider the Z_3-symmetric version of the superpotential, and therefore it contains no dimensional coupling.

In addition to the supersymmetric Lagrangian, the low-energy NMSSM contains the soft-SUSY-breaking terms,

$$\begin{aligned}
\mathcal{L}_{\text{soft}} = & - m_1^2 \Phi_d^\dagger \Phi_d - m_2^2 \Phi_u^\dagger \Phi_u - m_n^2 n^* n - m_{\tilde{q}}^2 \tilde{q}_L^\dagger \tilde{q}_L - m_{\tilde{d}}^2 \tilde{d}_R^\dagger \tilde{d}_R - m_{\tilde{u}}^2 \tilde{u}_R^\dagger \tilde{u}_R \\
& - \left\{ (f_d A_d) \Phi_d \tilde{q}_L \tilde{d}_R^* - (f_u A_u) \Phi_u \tilde{q}_L \tilde{u}_R^* - \lambda A_\lambda n \Phi_d \Phi_u + \text{h.c.} \right\} \\
& - \left(m_n' n^2 + \frac{1}{3} \kappa A_\kappa n^3 + \text{h.c.} \right),
\end{aligned} \tag{2·2}$$

where $\tilde{q}_L$, $\tilde{d}_R$ and $\tilde{u}_R$ are the squark fields, and Φ_d, Φ_u and n are the Higgs fields. Although the n^2 term breaks the global Z_3-symmetry, the n^2-term does not exist in the simple supergravity model. For this reason we do not include the n^2-term in the following. We assume that the values of all the dimensional parameters in $\mathcal{L}_{\text{soft}}$ are near weak scale.

In the case $\kappa = 0$, the global Z_3-symmetry is promoted to $U(1)$ PQ symmetry ($n \to e^{i\alpha}n$ and $\Phi_u \to e^{-i\alpha}\Phi_u$). Then the pseudoscalar component of the singlet becomes a Nambu-Goldstone (NG) mode when the singlet acquires a VEV. For small κ, the PQ symmetry is slightly broken, and a relatively light axion is expected.[14] The spontaneous breakdown of the global Z_3-symmetry causes the domain wall problem.[15] If we introduced Z_3-breaking linear or bilinear terms into the superpotential, this problem could be solved.[16] However, this inevitably results in the appearance of a dimensional parameter in the superpotential. Therefore we assume that this symmetry is broken at an early stage of the universe far before the EWPT by some higher-dimensional operator that becomes irrelevant at low energies.

The tree-level Higgs potential is composed of three parts, $V = V_F + V_D + V_{\rm soft}$:

$$V_F = |\lambda n|^2(\Phi_d^\dagger\Phi_d + \Phi_u^\dagger\Phi_u) + |\epsilon_{ij}\lambda\Phi_d^i\Phi_u^j + \kappa n^2|^2, \tag{2·3}$$

$$V_D = \frac{g_2^2+g_1^2}{8}(\Phi_d^\dagger\Phi_d - \Phi_u^\dagger\Phi_u)^2 + \frac{g_2^2}{2}(\Phi_d^\dagger\Phi_u)(\Phi_u^\dagger\Phi_d), \tag{2·4}$$

$$V_{\rm soft} = m_1^2\Phi_d^\dagger\Phi_d + m_2^2\Phi_u^\dagger\Phi_u + m_N^2|n|^2 - \left(\epsilon_{ij}\lambda A_\lambda n\Phi_d^i\Phi_u^j + \frac{1}{3}\kappa A_\kappa n^3 + \text{h.c.}\right). \tag{2·5}$$

Here, we expand this potential about the VEVs represented by v_d, v_u, v_n and the phases θ and φ. The parametrization of the scalar fields is as follows:

$$\Phi_d = \begin{pmatrix} \frac{1}{\sqrt{2}}(v_d + h_d + ia_d) \\ \phi_d^- \end{pmatrix}, \quad \Phi_u = e^{i\theta}\begin{pmatrix} \phi_u^+ \\ \frac{1}{\sqrt{2}}(v_u + h_u + ia_u) \end{pmatrix}, \tag{2·6}$$

$$n = \frac{1}{\sqrt{2}}e^{i\varphi}(v_n + h_n + ia_n). \tag{2·7}$$

The condition for the scalar potential to have an extremum at the vacuum is that the first derivatives with respect to the Higgs fields evaluated at the vacuum vanish:

$$0 = \frac{1}{v_d}\left\langle\frac{\partial V_0}{\partial h_d}\right\rangle = \tilde{m}_1^2 - R_\lambda\frac{v_u v_n}{v_d} + \frac{g_2^2+g_1^2}{8}(v_d^2 - v_u^2) + \frac{|\lambda|^2}{2}(v_u^2 + v_n^2) + \frac{\mathcal{R}}{2}\frac{v_u v_n^2}{v_d}, \tag{2·8}$$

$$0 = \frac{1}{v_u}\left\langle\frac{\partial V_0}{\partial h_u}\right\rangle = \tilde{m}_2^2 - R_\lambda\frac{v_d v_n}{v_u} - \frac{g_2^2+g_1^2}{8}(v_d^2 - v_u^2) + \frac{|\lambda|^2}{2}(v_d^2 + v_n^2) + \frac{\mathcal{R}}{2}\frac{v_d v_n^2}{v_u}, \tag{2·9}$$

$$0 = \frac{1}{v_n}\left\langle\frac{\partial V_0}{\partial h_N}\right\rangle = \tilde{m}_N^2 - R_\lambda\frac{v_d v_u}{v_n} - R_\kappa v_n + \frac{|\lambda|^2}{2}(v_d^2 + v_u^2) + |\kappa|^2 v_n^2 + \mathcal{R}v_d v_u, \tag{2·10}$$

$$0 = \frac{1}{v_u}\left\langle\frac{\partial V_0}{\partial a_d}\right\rangle = \frac{1}{v_d}\left\langle\frac{\partial V_0}{\partial a_u}\right\rangle = I_\lambda v_n - \frac{1}{2}\mathcal{I}v_n^2, \tag{2·11}$$

$$0 = \frac{1}{v_n}\left\langle\frac{\partial V_0}{\partial a_N}\right\rangle = I_\lambda\frac{v_d v_u}{v_n} + I_\kappa v_n + \mathcal{I}v_d v_u. \tag{2·12}$$

Here, we have

$$\mathcal{R} = \text{Re}[\lambda\kappa^* e^{i(\theta-2\varphi)}], \qquad \mathcal{I} = \text{Im}[\lambda\kappa^* e^{i(\theta-2\varphi)}], \tag{2·13}$$

$$R_\lambda = \frac{1}{\sqrt{2}}\mathrm{Re}[\lambda A_\lambda e^{i(\theta+\varphi)}], \qquad I_\lambda = \frac{1}{\sqrt{2}}\mathrm{Im}[\lambda A_\lambda e^{i(\theta+\varphi)}], \tag{2·14}$$

$$R_\kappa = \frac{1}{\sqrt{2}}\mathrm{Re}[\kappa A_\kappa e^{i3\varphi}], \qquad I_\kappa = \frac{1}{\sqrt{2}}\mathrm{Im}[\kappa A_\kappa e^{i3\varphi}], \tag{2·15}$$

and $\langle\cdots\rangle$ denotes the value evaluated at the vacuum. These conditions are called *tadpole conditions* in the sense that the conditions make the tadpole diagrams vanish if we set the Higgs fields to their VEVs. Note that $\mathcal{R}$ and $\mathcal{I}$ are dimensionless parameters and R_λ, R_κ, I_λ and I_κ have the dimension of mass. The phases appear only through the three combinations (2·13)–(2·15) given above. Hence, our formulation to this point does not depend on the convention for the phases. From (2·11) and (2·12), we obtain the two conditions

$$I_\lambda = \frac{1}{2}\mathcal{I}v_n, \quad I_\kappa = -\frac{3}{2}\mathcal{I}\frac{v_d v_u}{v_n}. \tag{2·16}$$

Because of the two tadpole conditions on the three CP violating parameters $\mathcal{I}$, I_λ and I_κ, only one of them is physical. When we introduce complex parameters, they must be chosen to satisfy the tadpole conditions (2·16).

2.2. *The mass and couplings of the Higgs scalars*

The mass matrix of the neutral Higgs scalars, which is defined using the second derivative of the Higgs potential evaluated at the vacuum, has the structure

$$\mathcal{M}^2 = \begin{pmatrix} \mathcal{M}_S^2 & \mathcal{M}_{SP}^2 \\ (\mathcal{M}_{SP}^2)^T & \mathcal{M}_P^2 \end{pmatrix}, \tag{2·17}$$

where the basis is $(\boldsymbol{h}^T\ \boldsymbol{a}^T) = (h_d\ h_u\ h_n\ a_d\ a_u\ a_n)$. Here, the block components of $\mathcal{M}^2$ are given by

$$\mathcal{M}_S^2 = \begin{pmatrix} R_\lambda v_n \tan\beta + m_Z^2\cos^2\beta & -R_\lambda v_n - m_Z^2\sin\beta\cos\beta & -R_\lambda v_u + |\lambda|^2 v_n v_d \\ -\frac{1}{2}\mathcal{R}v_n^2\tan\beta & +\frac{1}{2}\mathcal{R}v_n^2 + |\lambda|^2 v_d v_u & +\mathcal{R}v_n v_u \\ -R_\lambda v_n - m_Z^2\sin\beta\cos\beta & R_\lambda v_n\cot\beta + m_Z^2\sin^2\beta & -R_\lambda v_d + |\lambda|^2 v_n v_u \\ +\frac{1}{2}\mathcal{R}v_n^2 + |\lambda|^2 v_d v_u & -\frac{1}{2}\mathcal{R}v_n^2\cot\beta & +\mathcal{R}v_n v_d \\ -R_\lambda v_u + |\lambda|^2 v_n v_d & -R_\lambda v_d + |\lambda|^2 v_n v_u & R_\lambda\frac{v_d v_u}{v_n} - R_\kappa v_n \\ +\mathcal{R}v_n v_u & +\mathcal{R}v_n v_d & +2|\kappa|^2 v_n^2 \end{pmatrix}, \tag{2·18}$$

$$\mathcal{M}_P^2 = \begin{pmatrix} (R_\lambda - \mathcal{R}v_n/2)v_n\tan\beta & (R_\lambda - \mathcal{R}v_n/2)v_n & (R_\lambda + \mathcal{R}v_n)v_u \\ (R_\lambda - \mathcal{R}v_n/2)v_n & (R_\lambda - \mathcal{R}v_n/2)v_n\cot\beta & (R_\lambda + \mathcal{R}v_n)v_d \\ (R_\lambda + \mathcal{R}v_n)v_u & (R_\lambda + \mathcal{R}v_n)v_d & R_\lambda\frac{v_d v_u}{v_n} + 3R_\kappa v_n - 2\mathcal{R}v_d v_u \end{pmatrix}, \tag{2·19}$$

$$\mathcal{M}_{SP}^2 = \begin{pmatrix} 0 & 0 & \frac{3}{2}\mathcal{I}v_n v_u \\ 0 & 0 & \frac{3}{2}\mathcal{I}v_n v_d \\ -\frac{1}{2}\mathcal{I}v_n v_u & -\frac{1}{2}\mathcal{I}v_n v_d & -2\mathcal{I}v_d v_u \end{pmatrix}, \tag{2·20}$$

where we have used the tadpole conditions (2·8)–(2·10) and (2·16) to express the scalar soft masses and I_λ and I_κ in terms of the other parameters. In the following,

we also adopt the usual conventions $\tan\beta = v_u/v_d$ and $v^2 = v_d^2 + v_u^2$. It is worth emphasizing that if CP violation at the tree level is turned off (i.e. $\mathcal{I} = 0$), the scalar mass matrix becomes block diagonal.

The three pseudoscalars contain one NG mode, which is isolated by the β rotation

$$\boldsymbol{a} = U(\beta)\begin{pmatrix} G \\ \boldsymbol{a}' \end{pmatrix} = \begin{pmatrix} \cos\beta & \sin\beta & 0 \\ -\sin\beta & \cos\beta & 0 \\ 0 & 0 & 1 \end{pmatrix}\begin{pmatrix} G \\ a \\ a_n \end{pmatrix}, \tag{2·21}$$

where G is the NG mode which would be eaten up by the gauge bosons. After isolating the NG mode, the mass term of the neutral Higgs bosons is given by

$$\mathcal{L}_m = -\frac{1}{2}\begin{pmatrix} \boldsymbol{h}^T & \boldsymbol{a}'^T \end{pmatrix}\begin{pmatrix} \mathcal{M}_S^2 & \mathcal{M}_{SP}^{2\prime} \\ (\mathcal{M}_{SP}^{2\prime})^T & \mathcal{M}_P^{2\prime} \end{pmatrix}\begin{pmatrix} \boldsymbol{h} \\ \boldsymbol{a}' \end{pmatrix}, \tag{2·22}$$

where

$$\mathcal{M}_{SP}^{2\prime} = \begin{pmatrix} 0 & \frac{3}{2}\sin\beta \\ 0 & \frac{3}{2}\cos\beta \\ -\frac{1}{2} & -\sin 2\beta \end{pmatrix}\mathcal{I}v_n v, \tag{2·23}$$

$$\mathcal{M}_P^{2\prime} = \begin{pmatrix} (2R_\lambda - \mathcal{R}v_n)\frac{v_n}{\sin 2\beta} & (R_\lambda + \mathcal{R}v_n)v \\ (R_\lambda + \mathcal{R}v_n)v & \frac{R_\lambda}{2}\frac{v^2}{v_n}\sin 2\beta + 3R_\kappa v_n - \mathcal{R}v^2\sin 2\beta \end{pmatrix}. \tag{2·24}$$

The equations (2·23) and (2·24) demonstrate that one of the pseudoscalars is massless in the case $\kappa = 0$ ($\mathcal{I} = \mathcal{R} = R_\kappa = 0$). This is true even when we include radiative corrections. We define $\mathcal{M}'^2$ as the mass matrix of the neutral Higgs bosons after extracting the NG mode. Then the masses of the neutral Higgs bosons are obtained by diagonalizing the mass matrix $\mathcal{M}'^2$ through an orthogonal rotation $O^T\mathcal{M}'^2 O = \mathrm{diag}(m_{h_1}^2\ m_{h_2}^2\ m_{h_3}^2\ m_{h_4}^2\ m_{h_5}^2)$, where we define the matrix O in such a way that the eigenvalues satisfy

$$m_{h_1}^2 < m_{h_2}^2 < m_{h_3}^2 < m_{h_4}^2 < m_{h_5}^2. \tag{2·25}$$

Without CP violation (i.e., for $\mathcal{I} = 0$), the mass eigenstates are also CP eigenstates S_i and A_i, where A_i has vanishing g_{VVh} coupling. (V represents the W and Z bosons.)

Similarly, the charged Higgs mass $m_{H^\pm}$ is obtained through the β rotation of the charged Higgs mass matrix:

$$\begin{aligned} m_{H^\pm}^2 &= \frac{1}{\sin\beta\cos\beta}\left\langle \frac{\partial^2 V}{\partial\phi_d^+\partial\phi_u^-}\right\rangle \\ &= m_W^2 - \frac{1}{2}|\lambda|^2 v^2 + (2R_\lambda - \mathcal{R}v_n)\frac{v_n}{\sin 2\beta}. \end{aligned} \tag{2·26}$$

We use this equation in order to substitute $m_{H^\pm}$ for R_λ using the relation

$$R_\lambda = \frac{1}{2}\hat{m}^2\frac{\sin 2\beta}{v_n} + \frac{1}{2}\mathcal{R}v_n, \tag{2·27}$$

where

$$\hat{m}^2 \equiv m_{H^\pm}^2 - m_W^2 + \frac{1}{2}|\lambda|^2 v^2. \tag{2·28}$$

For example, the CP-odd components of the mass matrix are written

$$\mathcal{M}_P^{2\prime} = \begin{pmatrix} \hat{m}^2 & \frac{1}{2}\hat{m}^2\frac{v}{v_n}\sin 2\beta + \frac{3}{2}\mathcal{R}v_n v \\ \frac{1}{2}\hat{m}^2\frac{v}{v_n}\sin 2\beta + \frac{3}{2}\mathcal{R}v_n v & \frac{1}{4}\hat{m}^2(\frac{v}{v_n}\sin 2\beta)^2 - \frac{3}{4}\mathcal{R}v^2\sin 2\beta + 3\mathcal{R}_\kappa v_n \end{pmatrix}. \tag{2·29}$$

Now we have seven mass eigenstates, but we have no obvious bounds on the eigenvalues, like the upper (lower) bound on the lightest (heaviest) Higgs scalar in the MSSM at the tree level. Instead, without CP violation, the inequality $\det\left(\hat{m}^2 - \mathcal{M}_P^{2\prime}\right) < 0$ implies that $m_{A_1}^2 < \hat{m}^2 < m_{A_2}^2$. It is difficult to derive such inequality for the CP-even scalars, but in the limit that $\hat{m}^2 \gg v_0^2, v_n^2$, we have the approximate relation $\det\left(\hat{m}^2 - \mathcal{M}_S^2\right) \lesssim 0$, which implies that $m_{S_1}^2 < m_{S_2}^2 < \hat{m}^2 < m_{S_3}^2$. These relations account for the relations among the mass eigenvalues in the case of heavy charged Higgs boson, with the help of $\mathrm{Tr}\mathcal{M}_S^2$ and $\mathrm{Tr}\mathcal{M}_P^2$, which constrain the sum of the masses.

Although the singlet Higgs fields h_n and a_n do not couple to the gauge bosons, all the mass eigenstates of the neutral Higgs boson can interact with the W, Z bosons and fermions, because the singlet fields are mixed with the doublet fields. The couplings of the charged Higgs boson with the gauge bosons and quarks are identical to those in the MSSM. In particular, the VVh-, Zhh- and bbh-vertices are important for the study of Higgs production and decay events in colliders.[2)] In a LEP-type e^+e^- collider, the dominant production processes of the neutral Higgs bosons are the Higgs strahlung process associated with the Z boson, the W-fusion production process, and the pair production processes if $m_{h_1} + m_{h_2} < \sqrt{s}$. For the decay of a light Higgs boson, $h \to b\bar{b}$ is the main mode, with the subleading $h \to \tau^+\tau^-$ mode. In both cases, the correction factors to the relevant Yukawa couplings are the same, and they characterize the deviation from the MSM. In addition to the above-cited processes, the gluon fusion process and the Yukawa process are important in high-energy hadron collider experiments.[17)]

It is straightforward to read off the vertices from the kinetic terms of the Higgs bosons and from the Yukawa coupling terms. We find

$$\mathcal{L}_{VVh} = g_2 m_W g_{VVh_i}\left(W_\mu^+ W^{-\mu} + \frac{1}{2\cos^2\theta_W}Z_\mu Z^\mu\right)h_i, \tag{2·30}$$

$$\begin{aligned}\mathcal{L}_{Zhh} &= \frac{g_2}{2\cos\theta_W}(h_d \overleftrightarrow{\partial}_\mu a_d - h_u \overleftrightarrow{\partial}_\mu a_u)Z^\mu \\ &= \frac{g_2}{2\cos\theta_W}g_{Zh_ih_j}Z^\mu(h_i \overleftrightarrow{\partial}_\mu h_j),\end{aligned} \tag{2·31}$$

$$\mathcal{L}_{bbh} = -\frac{g_2 m_b}{2m_W}\bar{b}(g_{bbh_i}^S + i\gamma^5 g_{bbh_i}^P)bh_i, \tag{2·32}$$

where the correction factors to the couplings are

$$g_{VVh_i} = O_{1i}\cos\beta + O_{2i}\sin\beta, \tag{2·33}$$

$$g_{Zh_ih_j} = \frac{1}{2}\left\{(O_{4i}O_{2j} - O_{4j}O_{2i})\cos\beta - (O_{4i}O_{1j} - O_{4j}O_{1i})\sin\beta\right\}, \tag{2·34}$$

$$g_{bbh_i}^S = O_{1i}\frac{1}{\cos\beta}, \quad g_{bbh_i}^P = -O_{4i}\tan\beta. \tag{2·35}$$

Thus, the mass eigenstates and the gauge eigenstates are related as $h_d = O_{1i}h_i$, $h_u = O_{2i}h_i$ and $a = O_{4i}h_i$, where i is summed from 1 to 5. The Zh_ih_j coupling vanishes for $i = j$, because of its antisymmetric derivative form. This coupling also vanishes when both the Higgs bosons are either scalars ($i, j = 1, 2, 3$) or pseudoscalars ($i, j = 4, 5$). However, we believe that all the $g_{Zh_ih_j}$ have nonzero values in the CP-violating case, because of the mixing of these CP eigenstates. The equations (2·33)–(2·35) have the same structure as the corresponding equations in the MSSM,[8] except for the mixing including the singlet.

2.3. *Constraints on the parameters*

The NMSSM has more parameters than the MSSM. Our main concern is to search for allowed parameter values in the case of a weak scale v_n, for which we expect there to appear new features in the spectrum and coupling of the Higgs bosons, as well as phase transitions at finite temperature. In order to determine the allowed parameters, we impose the following two conditions on the model:

(1) The vacuum condition, which requires that prescribed vacuum be the global minimum of the effective potential. This also requires that all the masses-squared of the scalars including the sfermions be positive.
(2) The spectrum condition, which requires that the mass of the Higgs boson with its couplings to the vector boson $|g_{VVh}|$ larger than 0.1 be heavier than the bound 114 GeV.

The constraint on the gauge coupling is the most stringent, and for this reason we examine the other couplings for the allowed parameters later. Because the mass matrix of the Higgs bosons is subject to large radiative corrections, we need numerical studies to determine the results of the spectrum condition. Such results are presented in §4. Here we attempt to find an analytic form of the constraints obtained from the vacuum condition at the tree level.

In the MSSM, the global minimum of the tree-level potential is always located at the vacuum, as long as the D-flat direction is lifted by the soft terms and the tadpole conditions are satisfied. Although the Higgs potential in the NMSSM is bounded from below by the F-terms, the prescribed vacuum is not always the global minimum of the potential, even when the tadpole conditions are satisfied. This is because the trilinear terms in $\mathcal{L}_{\rm soft}$, which give negative contributions to the potential, cause the global minimum to appear at some point other than the vacuum. We must exclude sets of parameter values that yield such an unwanted global minimum. A necessary condition for the correct vacuum is that the mass-squared of all the scalars be positive. In the CP-conserving case, applying this condition to the pseudoscalars implies that $\det {\mathcal{M}'_P}^2 > 0$. Hence we have

$$\hat{m}^2 \left(-\frac{3}{4}\mathcal{R}v^2 \sin 2\beta + R_\kappa v_n \right) > \frac{3}{4}\mathcal{R}^2 v^2 v_n^2. \tag{2·36}$$

This requires that each factor on the left-hand side has the same sign, and it gives a lower bound on the charged scalar mass, which must be large enough in the case that $\hat{m}^2 > 0$.

Another necessary condition is that the value of the scalar potential at the prescribed vacuum be smaller than that at the origin. At the tree level, $V(0)$ is zero and $V|_{\rm vacuum}$ is

$$V|_{\rm vacuum} = -\frac{1}{4}|\lambda|^2 v_n^2 v^2 - \frac{1}{4}|\kappa|^2 v_n^4 - \frac{1}{8}m_Z^2 v^2 \cos^2 2\beta - \frac{1}{8}m_W^2 v^2 \sin^2 2\beta + \frac{1}{8}m_{H^\pm}^2 v^2 \sin^2 2\beta - \frac{1}{8}\mathcal{R} v_n^2 v^2 \sin 2\beta + \frac{1}{6}R_\kappa v_n^3, \tag{2·37}$$

where we have used the tadpole conditions (2·8)–(2·10) to eliminate the soft masses of the Higgs fields and have used $m_{H^\pm}$ instead of R_λ. Then, requiring $V|_{\rm vacuum} < 0$ yields the following condition on $m_{H^\pm}$:

$$m_{H^\pm}^2 < 2|\lambda|^2 v_n^2 \frac{1}{\sin^2 2\beta} + 2|\kappa|^2 \frac{v_n^4}{v^2}\frac{1}{\sin^2 2\beta} + m_Z^2 \cot^2 2\beta + m_W^2 + \mathcal{R} v_n^2 \frac{1}{\sin 2\beta} - \frac{4}{3}R_\kappa \frac{v_n^3}{v^2}\frac{1}{\sin^2 2\beta}. \tag{2·38}$$

This bound holds whether there is CP violation or not. The charged Higgs mass $m_{H^\pm}$ is not constrained in the MSSM-limit in which λv_n and κv_n are fixed for $v_n \to \infty$,[6] due to the effect of the infinitely large v_n^4 term. Therefore the above condition is important in the pure-NMSSM parameter set, i.e., the case in which v_n is not large and λ and κ are not small. Figure 1 displays the tree-level charged Higgs mass bounds for an example of a pure-NMSSM parameter set. The solid curve, which represents the upper bound, suggests that the charged Higgs boson must be lighter than 400 GeV. Hence the pure-NMSSM parameter set predicts that the charged Higgs boson possesses a mass that can be measured by the LHC.[18] The dashed curve represents the lower bound on the charged Higgs boson. It ends near $A_\kappa = 0$

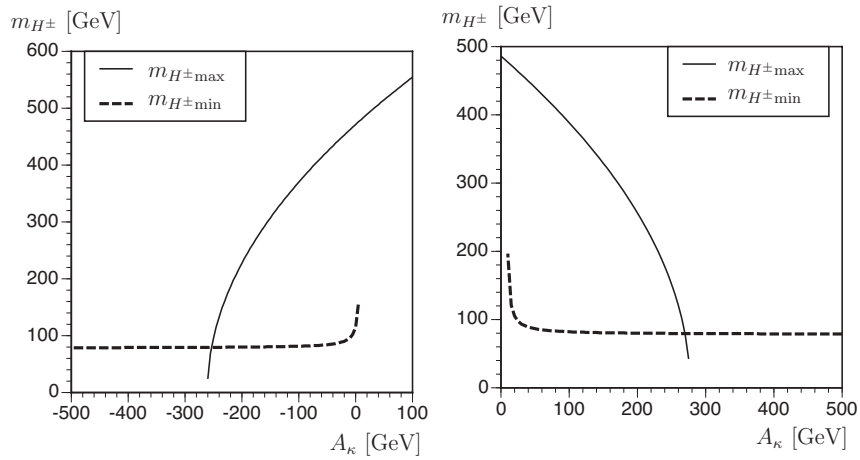

Fig. 1. The tree-level bounds on the mass of the charged Higgs boson as a function of A_κ for $\tan\beta = 5$, $v_n = 300$ GeV, $\lambda = 0.1$ and $\kappa = -0.3$ (left-hand plot) and $\kappa = 0.3$ (right-hand plot). The solid curve represents the upper mass bound of the charged Higgs boson and dashed curve represents the lower bound.

because near there the left-hand side of (2·36) becomes negative. The consistency of the model implies both upper and lower bounds on A_κ, which are on the order of the weak scale for a weak scale v_n. In particular, the situation in which κ and A_κ have the same sign is favored.

Once we fix $m_{H^\pm}$ and A_κ, the condition (2·38) excludes the elliptic region in the (λ, κ)-plane, whose area vanishes in the MSSM-limit. As we see below, this excludes a large portion of the parameter space for the case of a weak scale v_n.

§3. One-loop effective potential

We now evaluate the one-loop contributions to the tadpole conditions and the spectrum of the Higgs bosons. As mentioned in the previous section, the basic idea is almost the same as that in the tree-level analysis, and therefore we only present the results here. We analyze the effective potential of the Higgs fields taking into account the one-loop contributions from the gauge bosons and the third generation of the quarks and squarks. The corrections from the leptons and the other quarks and squarks can be ignored, because of their small Yukawa couplings to the Higgs fields. The corrections to the Higgs potential are given by

$$\Delta V = \Delta_q V + \Delta_{\tilde{q}} V + \Delta_g V, \tag{3·1}$$

where

$$\Delta_q V = -\frac{N_C}{16\pi^2} \sum_{q=t,b} \left(\bar{m}_q^2\right)^2 \left(\log \frac{\bar{m}_q^2}{M^2} - \frac{3}{2} \right), \tag{3·2}$$

$$\Delta_{\tilde{q}} V = \frac{N_C}{32\pi^2} \sum_{q=t,b} \sum_{j=1,2} \left(\bar{m}_{\tilde{q}_j}^2\right)^2 \left(\log \frac{\bar{m}_{\tilde{q}_j}^2}{M^2} - \frac{3}{2} \right), \tag{3·3}$$

$$\Delta_g V = \frac{3}{64\pi^2} \left[\left(\bar{m}_Z^2\right)^2 \left(\log \frac{\bar{m}_Z^2}{M^2} - \frac{3}{2} \right) + 2 \left(\bar{m}_W^2\right)^2 \left(\log \frac{\bar{m}_W^2}{M^2} - \frac{3}{2} \right) \right]. \tag{3·4}$$

The field-dependent masses $\bar{m}_X^2$ are listed in Appendix A. The tadpole conditions and the mass matrix are obtained by calculating the derivatives of the effective potential at the vacuum with these corrections. In particular, the imaginary parts of the tadpole conditions are

$$I_\lambda + \Delta I_\lambda = \frac{1}{2} \mathcal{I} v_n, \quad I_\kappa = -\frac{3}{2} \mathcal{I} \frac{v_d v_u}{v_n}, \tag{3·5}$$

where I_κ does not undergo a loop correction at this level. The correction ΔI_λ comes from the squark loops,

$$\Delta I_\lambda = \frac{N_C}{16\pi^2} \sum_{q=t,b} |y_q|^2 I_q \left[f(m_{\tilde{q}_1}^2, m_{\tilde{q}_2}^2) - 1 \right] v_n, \tag{3·6}$$

where I_q is defined by (A·10), and we have

$$f(m_1^2, m_2^2) = \frac{1}{\Delta m^2} \left[m_1^2 \left(\log \frac{m_1^2}{M^2} - 1 \right) - m_2^2 \left(\log \frac{m_2^2}{M^2} - 1 \right) \right], \tag{3·7}$$

with $\Delta m^2 = m_1^2 - m_2^2$.

Here we present the corrections to the mass matrix in detail. The couplings to the gauge bosons and the quarks are subject to the loop effects through the orthogonal matrix O, which is determined from the corrections to the neutral mass matrix $\mathcal{M}$. The scalar part $\mathcal{M}_S^2$ of the neutral mass matrix contains the loop contributions,

$$\Delta\mathcal{M}_S^2 = \Delta_q\mathcal{M}_S^2 + \Delta_g\mathcal{M}_S^2 + \Delta_{\tilde{q}}\mathcal{M}_S^2, \tag{3·8}$$

from the quarks, gauge bosons and squarks. The quark loops and gauge loops contribute only to the elements in the upper-left 2×2 submatrix, explicitly,

$$\Delta_q\mathcal{M}_S^2 = -\frac{N_C}{4\pi^2}\begin{pmatrix} |y_b|^2 m_b^2 \log\frac{m_b^2}{M^2} & 0 & 0 \\ 0 & |y_t|^2 m_t^2 \log\frac{m_t^2}{M^2} & 0 \\ 0 & 0 & 0 \end{pmatrix}, \tag{3·9}$$

$$\Delta_g\mathcal{M}_S^2 = \frac{3}{32\pi^2}\left(m_Z^2 \log\frac{m_Z^2}{M^2} + 2m_W^2 \log\frac{m_W^2}{M^2}\right)\begin{pmatrix} \cos^2\beta & \cos\beta\sin\beta & 0 \\ \cos\beta\sin\beta & \sin^2\beta & 0 \\ 0 & 0 & 0 \end{pmatrix}, \tag{3·10}$$

because they do not couple to the singlet in the tree-level potential. The squark-loop contributions are

$$\Delta_{\tilde{t}}\mathcal{M}_S^2 = \frac{N_C}{16\pi^2}\left[\mathcal{T}^S f(m_{\tilde{t}_1}^2, m_{\tilde{t}_2}^2) + \sum_{j=1,2}\left\langle\frac{\partial\bar{m}_{\tilde{t}_j}^2}{\partial \boldsymbol{h}}\right\rangle\left\langle\frac{\partial\bar{m}_{\tilde{t}_j}^2}{\partial \boldsymbol{h}}\right\rangle^T \log\frac{m_{\tilde{t}_j}^2}{M^2}\right], \tag{3·11}$$

$$\Delta_{\tilde{b}}\mathcal{M}_S^2 = \frac{N_C}{16\pi^2}\left[\mathcal{B}^S f(m_{\tilde{b}_1}^2, m_{\tilde{b}_2}^2) + \sum_{j=1,2}\left\langle\frac{\partial\bar{m}_{\tilde{b}_j}^2}{\partial \boldsymbol{h}}\right\rangle\left\langle\frac{\partial\bar{m}_{\tilde{b}_j}^2}{\partial \boldsymbol{h}}\right\rangle^T \log\frac{m_{\tilde{b}_j}^2}{M^2}\right], \tag{3·12}$$

where the matrices $\mathcal{T}$ and $\mathcal{B}$ and the list of derivatives of the field-dependent masses are given in Appendix B.

The quantities $\mathcal{M}_P^2$ and $\mathcal{M}_{SP}^2$ are not affected by the quark and gauge loops, but they contain contributions from squark loops,

$$\Delta\mathcal{M}_P^2 = \Delta_{\tilde{q}}\mathcal{M}_P^2, \quad \Delta\mathcal{M}_{SP}^2 = \Delta_{\tilde{q}}\mathcal{M}_{SP}^2, \tag{3·13}$$

where the squark-loop contributions are

$$\Delta_{\tilde{t}}\mathcal{M}_P^2 = \frac{N_C}{16\pi^2}\left[\mathcal{T}^P f(m_{\tilde{t}_1}^2, m_{\tilde{t}_2}^2) + \sum_{j=1,2}\left\langle\frac{\partial\bar{m}_{\tilde{t}_j}^2}{\partial \boldsymbol{a}}\right\rangle\left\langle\frac{\partial\bar{m}_{\tilde{t}_j}^2}{\partial \boldsymbol{a}}\right\rangle^T \log\frac{m_{\tilde{t}_j}^2}{M^2}\right], \tag{3·14}$$

$$\Delta_{\tilde{b}}\mathcal{M}_P^2 = \frac{N_C}{16\pi^2}\left[\mathcal{B}^P f(m_{\tilde{b}_1}^2, m_{\tilde{b}_2}^2) + \sum_{j=1,2}\left\langle\frac{\partial\bar{m}_{\tilde{b}_j}^2}{\partial \boldsymbol{a}}\right\rangle\left\langle\frac{\partial\bar{m}_{\tilde{b}_j}^2}{\partial \boldsymbol{a}}\right\rangle^T \log\frac{m_{\tilde{b}_j}^2}{M^2}\right], \tag{3·15}$$

and

$$\Delta_{\tilde{t}}\mathcal{M}_{SP}^2 = \frac{N_C}{16\pi^2}\left[-\mathcal{T}^{SP} f(m_{\tilde{t}_1}^2, m_{\tilde{t}_2}^2) + \sum_{j=1,2}\left\langle\frac{\partial\bar{m}_{\tilde{t}_j}^2}{\partial \boldsymbol{h}}\right\rangle\left\langle\frac{\partial\bar{m}_{\tilde{t}_j}^2}{\partial \boldsymbol{a}}\right\rangle^T \log\frac{m_{\tilde{t}_j}^2}{M^2}\right], \tag{3·16}$$

$$\Delta_{\tilde{b}}\mathcal{M}^2_{SP} = \frac{N_C}{16\pi^2}\left[-\mathcal{B}^{SP} f(m^2_{\tilde{b}_1}, m^2_{\tilde{b}_2}) + \sum_{j=1,2}\left\langle \frac{\partial \bar{m}^2_{\tilde{b}_j}}{\partial \boldsymbol{h}}\right\rangle \left\langle \frac{\partial \bar{m}^2_{\tilde{b}_j}}{\partial \boldsymbol{a}}\right\rangle^T \log\frac{m^2_{\tilde{b}_j}}{M^2}\right]. \quad (3\cdot17)$$

The NG mode can be extracted from $\mathcal{M}^2_P$ and $\mathcal{M}^2_{SP}$ with the same orthogonal transformation as at the tree level. The loop contributions to the off-diagonal matrix $\mathcal{M}^2_{SP}$ are proportional to the CP-violating parameters in the squark sector, I_q, which is defined in (A·10).

The charged Higgs mass is not affected by the singlet field, but it contains contributions from the gauge, quark and squark loops,

$$\Delta m^2_{H^\pm} = \Delta_g m^2_{H^\pm} + \Delta_q m^2_{H^\pm} + \Delta_{\tilde{q}} m^2_{H^\pm}, \quad (3\cdot18)$$

where the detailed form of each term is given in Appendix C of Ref. 13), except that μ in the MSSM is replaced by $\lambda v_n e^{i\varphi}/\sqrt{2}$. The quantity R_λ, which is determined from Eq. (2·27), undergoes loop corrections through the corrections to the charged Higgs mass.

§4. Parameter search

In this section, we report the results of a numerical search for the allowed parameter region with the one-loop corrections in the CP-conserving case. The allowed parameter sets are determined by requiring the two conditions discussed in §2.3. For this purpose, we scanned parameter values in the Higgs sector within the region defined as follows: $\tan\beta = 3$ – 20, $v_n = 100$ – 1000 GeV, $100 \le m_{H^\pm} \le 5000$ GeV and $-1000 \le A_\kappa \le 0$ GeV. Because we can always make λ positive, without loss of generality, the (λ, κ)-plane was scanned over the region defined by the relations $0 \le \lambda \le 1$ and $-1 \le \kappa \le 1$. For the squark sector, we adopt a small value of the A-term, specifically, $A_t = A_b = 20$ GeV, so that the squark fields do not acquire nonzero VEVs and three cases for the soft masses: the heavy-squark scenario with $(m_{\tilde{q}},\ m_{\tilde{t}_R}) = (1000\text{ GeV},\ 800\text{ GeV})$, the light-squark-1 with $(m_{\tilde{q}},\ m_{\tilde{t}_R}) = (1000\text{ GeV},\ 10\text{ GeV})$ and the light-squark-2 with $(m_{\tilde{q}},\ m_{\tilde{t}_R}) = (500\text{ GeV},\ 10\text{ GeV})$, where $m_{\tilde{q}}$ ($m_{\tilde{t}_R}$) denotes the doublet (singlet) soft mass. For simplicity, we set $m_{\tilde{b}_R} = m_{\tilde{t}_R}$. First, we consider a set of values for all parameters except λ and κ and exclude the regions in (λ, κ)-plane where the effective potential at the origin is smaller than that at the vacuum and the spectrum condition is not satisfied. Within the remaining region, we carried out a numerical search for the global minimum of the effective potential and excluded the points for which the minimum is located somewhere other than the vacuum.

In Fig. 2, we present a typical example of the allowed parameter region for $\tan\beta = 3$, $v_n = 200$ GeV, $m_{H^\pm} = 400$ GeV and $A_\kappa = -200$ GeV in the heavy-squark scenario. The white region indicates the allowed parameter region in the (λ, κ)-plane. Although negative κ is favored for negative A_κ, as mentioned in §2.3, we study the range of κ from -1 to 1, because it is not excluded completely. Within the dark gray elliptic region, the effective potential at the origin is smaller than that at the prescribed vacuum. This is predicted by (2·38), which was derived from the tree-

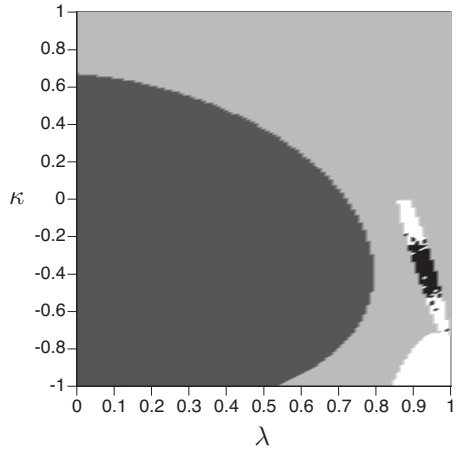

Fig. 2. Allowed parameter region as a function of λ and κ for $\tan\beta = 3$, $v_n = 200$ GeV, $m_{H^\pm} = 400$ GeV and $A_\kappa = -200$ GeV in the heavy-squark scenario. The allowed parameter region is the white region.

level potential. The broad, light gray region is excluded by the spectrum condition. Within the upper allowed region near $\kappa = 0$, the light Higgs scenario is realized, while in the lower allowed region, the lightest Higgs boson is heavier than 114 GeV. The narrow black region to the right of the elliptic one is excluded, because in that case, the global minimum is located at a point that is not the prescribed vacuum. For these excluded parameter values, the global minimum is located at $v = 0$, with large v_n, which depends on m_N^2, R_κ and $|\kappa|^2$.

We now explain the dependence of the allowed regions on the parameters. In Fig. 3, we make the same plot as in Fig. 2, but with (a) $v_n = 500$ GeV, (b) $A_\kappa = 500$ GeV, (c) light-squark-2 scenario and (d) $\tan\beta = 5$ and $m_{H^\pm} = 600$ GeV. As shown in Fig. 3(a), as v_n increases, the allowed region for the light Higgs shrinks, and the allowed region of the heavy Higgs spreads to small λ values. An allowed parameter set with small λ corresponds to the MSSM limit. Although not shown in the graph, similar behavior is observed when the charged Higgs boson becomes heavier. As A_κ increases, the allowed region becomes smaller. This is shown in Fig. 3(b), and it is also expected from Fig. 1. If we choose small $m_{\tilde{q}}$ and $m_{\tilde{q}_R}$, Fig. 3(c) and the same plot for the light-squark-2 scenario exhibit weak dependence on the squark soft masses. Figure 3(d) indicates that as $\tan\beta$ increases, the allowed region with light Higgs becomes narrower. At $\tan\beta = 20$, the allowed region is point-like at $\kappa = 0$, where one of the pseudoscalar is always massless.

Now, we consider the details of the Higgs mass spectrum and couplings. In Figs. 4 and 5, we display the behavior of the Higgs masses (Fig. 4, left) and the couplings of the three lightest Higgs bosons to the massive gauge bosons (Fig. 4, right) and to the bottom quarks (Fig. 5, left), and the Zhh-couplings (Fig. 5, right) as functions of κ for the same parameter values as in Fig. 2, with $\lambda = 0.9$. These correction factors to the coupling constants are defined in (2·33)–(2·35). As seen from Fig. 2, the allowed region along $\lambda = 0.9$ is divided into two parts, one of which

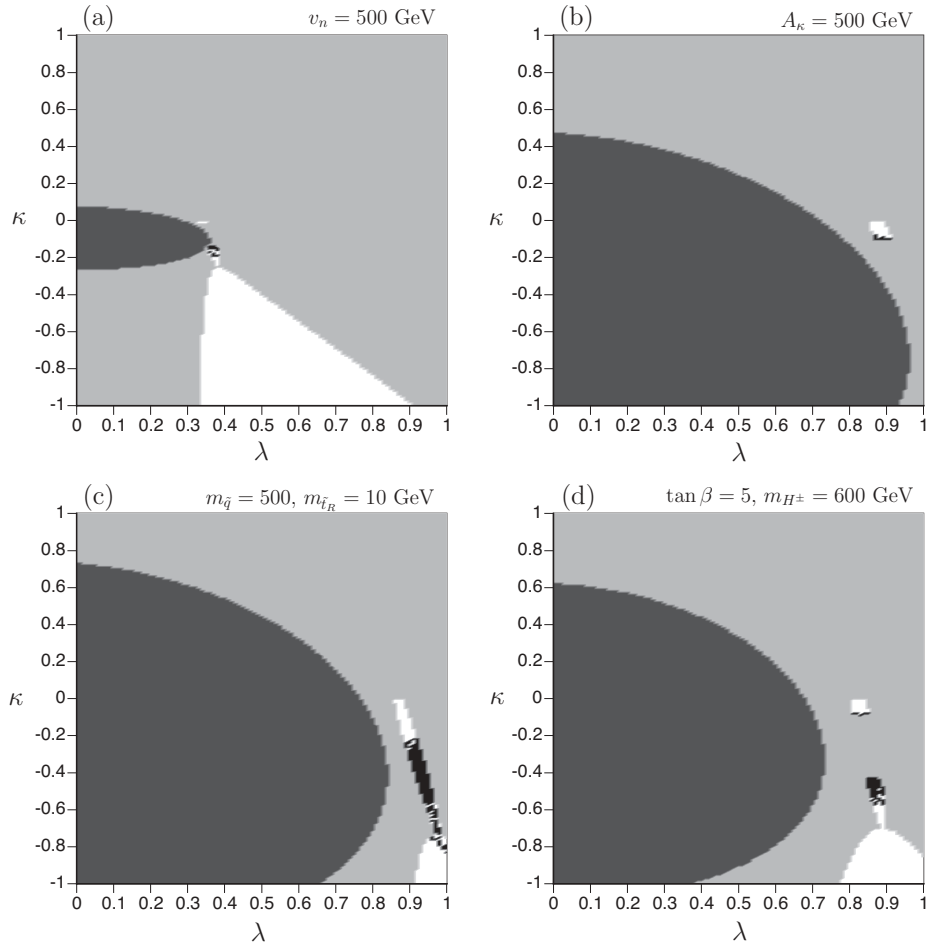

Fig. 3. The same as Fig. 2, but with (a) $v_n = 500$ GeV, (b) A_κ=500 GeV, (c) light-squark-2 scenario (i.e. $m_{\tilde{q}} = 500$ GeV, $m_{\tilde{t}_R} = 10$ and $A_t = 20$ GeV) and (d) $\tan\beta = 5$ and $m_{H^\pm} = 600$ GeV.

corresponds to the light Higgs scenario with small $|\kappa|$. The range of values of κ satisfying the spectrum condition can be read from Fig. 4 to be $-0.33 < \kappa < -0.05$, some part of which is excluded by the vacuum condition. Within the other allowed region, for $-1.0 < \kappa < -0.8$, all the Higgs bosons are heavier than 114 GeV. We refer to such sets of parameter values as the heavy Higgs scenario. In the scenario, the relatively heavy Higgs boson h_3 is almost decoupled from the theory, because its couplings g_{VVh_3} and g_{bbh_3} are small. The lighter two Higgs bosons are both CP-even scalars. Hence, in this scenario, the NMSSM behaves like the MSSM. In particular, the lightest Higgs boson is heavier than 120 GeV, and its coupling to the bottom quark is not so large, $g^2_{bbh_1} < 2.2$, which is outside the experimental bounds, as also is the case for the MSSM. We thus find that it is difficult to distinguish the NMSSM from the MSSM in the heavy Higgs scenario.

In the light Higgs scenario, light Higgs bosons cannot be observed in collider

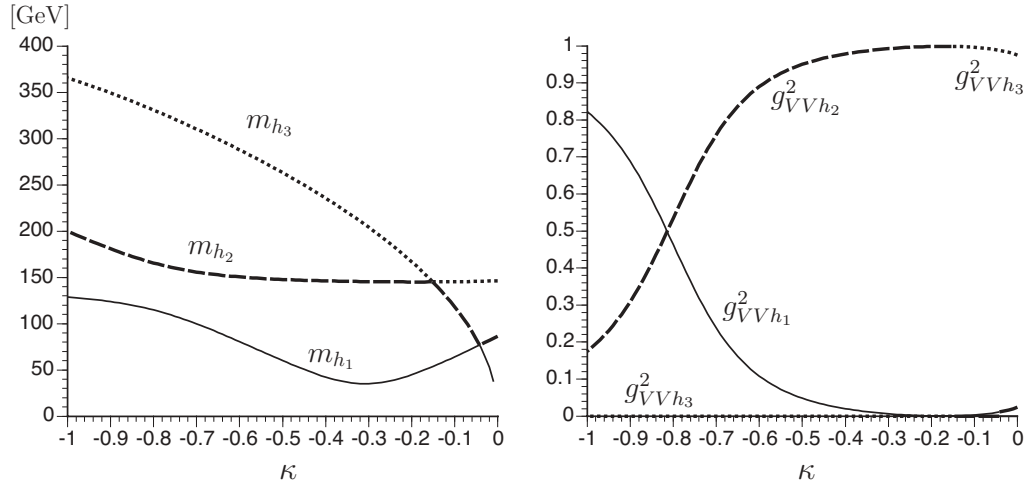

Fig. 4. The Higgs masses (left) and couplings (right) to the V-bosons as functions of κ for the same parameter values as in Fig. 2 with $\lambda = 0.9$. In the left plot, the solid curve, broken curve and dotted curve represent m_{h_1}, m_{h_2} and m_{h_3}, respectively. In the right plot, the solid curve, dashed curve and dotted curve represent $g^2_{VVh_1}$, $g^2_{VVh_2}$ and $g^2_{VVh_2}$, respectively.

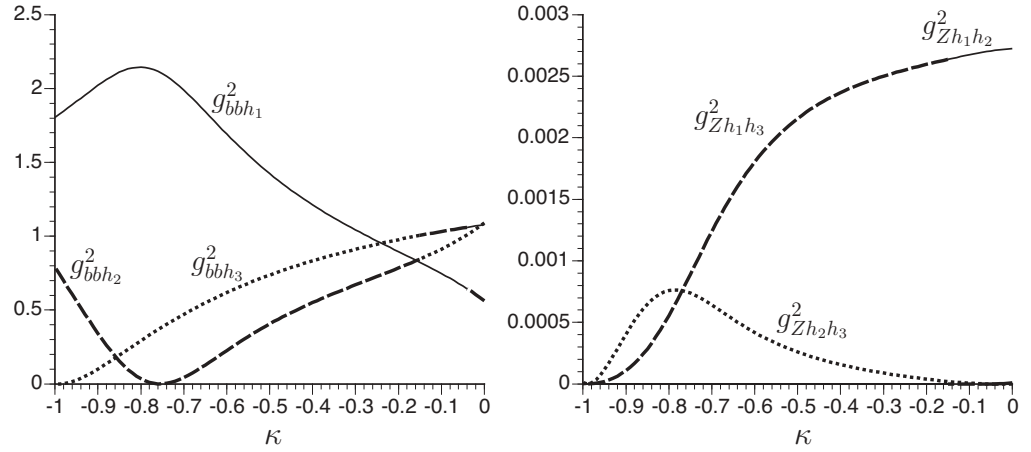

Fig. 5. The couplings of the three lightest Higgs bosons to the bottom quarks and the Z boson as functions of κ for the same parameters as in Fig. 4. In the left plot, the solid curve, broken curve and dotted curve represent $g^2_{bbh_1} = (g^S_{bbh_1})^2 + (g^P_{bbh_1})^2$, $g^2_{bbh_2}$ and $g^2_{bbh_3}$, respectively. In the right plot, the solid curve, broken curve and dotted curve represent $g^2_{Zh_1h_2}$, $g^2_{Zh_1h_3}$ and $g^2_{Zh_2h_3}$, respectively.

experiments. The main processes for producing Higgs bosons at the LEP 2 are the Higgs strahlung process and the W-fusion process, but both processes include small VVh-couplings (shown in the right plot of Fig. 4) and are not capable of producing light Higgs bosons. Though pair production becomes important when the total mass of the lightest scalar and the lightest pseudoscalar bosons is under the LEP 2 threshold, they cannot be created as a pair[19] because the coupling $g^2_{Zh_1h_3}$ ($g^2_{Zh_1h_2}$), shown in the right plot of Fig. 5, is too small. The Yukawa processes could

be dominant where these processes are suppressed, but the Yukawa processes cannot be observed unless the bbh-couplings are fairly large.[20] In the left plot of Fig. 5, the Yukawa couplings g_{bbh} are almost unity in the light Higgs region. With these couplings, the light Higgs bosons h_1 and h_2 produced in the Yukawa processes are likely to be unobservable. The situation is essentially the same even if we consider hadron colliders. The SM-Higgs search experiments at the Tevatron mainly consider the strahlung process with $W(Z)$ in the low mass range $110 < m_h < 140\,\mathrm{GeV}$, and the results show that the signal efficiency is too small to observe a Higgs boson.[21] At the LHC, the gluon fusion and the W fusion processes become important. Though h_1 and h_2 production in the W fusion process is suppressed by their small gauge couplings, their production in the gluon fusion process is not suppressed. However, it is in general difficult to distinguish gluon fusion events from the background, because the process produces the Higgs boson only. Therefore, it is expected that h_3 will first be detected in collider experiments. In this case, the model is very similar to the SM with a Higgs mass that can be as large as 150 GeV.

§5. Effects of the CP violation

Now we turn to CP violation and study its effects on the spectrum and gauge couplings of the Higgs bosons. Such an analysis is carried out in Ref. 8) for MSSM by considering CP violation in the squark sector. Here we focus on tree-level CP violation, which does not exist in the MSSM and is characterized by the parameter $\mathcal{I}$ defined in (2·13). In addition to $\mathcal{I}$, the complex parameters in the Higgs sector entering the mass-squared matrix are included in $\mathcal{R}$, R_λ and R_κ. When all the parameters are real, as in the previous section, one can freely assign their values. However, if some of them are complex, we must choose the parameters and the phases θ and φ in such a way to satisfy the tadpole conditions (3·5). Before presenting the numerical results, we explain how we parameterize the CP violation.

First, R_λ is fixed by the charged Higgs mass $m_{H^\pm}$ from the equations (2·27) and (3·18). The remaining parameters, $\mathcal{R}$, R_κ and $\mathcal{I}$, are determined by λ, κ, A_κ, θ and φ. Here, λ, κ and A_κ are complex numbers, and some of the phases are redundant. We denote the phases of λ, κ and A_κ by δ_λ, δ_κ and δ_{A_κ}, respectively. Among these, the independent phases are collected into $\delta'_\kappa \equiv \delta_\kappa + 3\varphi$, δ_{A_κ} and $\delta_{\mathrm{EDM}} \equiv \delta_\lambda + \theta + \varphi$. The phase δ_{EDM} is effective to nEDM if the gaugino masses and A_q are real. The counterpart to δ_{EDM} in the MSSM is the phase of the μ-parameter plus θ. Suppose that we first choose $|\lambda|$, $|\kappa|$, δ_{EDM} and δ'_κ, from which $\mathcal{R}$ and $\mathcal{I}$ are determined. Because I_κ is fixed by (3·5), the absolute value of A_κ can be chosen freely, but not the phase. In particular, R_κ is determined, without specifying δ_{A_κ}, by the relation

$$R_\kappa^2 = \frac{1}{2}|\kappa A_\kappa|^2 - I_\kappa^2 = \frac{1}{2}|\kappa A_\kappa|^2 - \left(\frac{3\mathcal{I} v_d v_u}{2 v_n}\right)^2, \tag{5·1}$$

where we have used the second equation in (3·5). Note that $|\kappa A_\kappa|$ must be larger than $3\mathcal{I} v_d v_u/\sqrt{2} v_n$ in order for (5·1) to have a real solution for R_κ. In the following, we adopt the phase convention so that the phase relevant to the nEDM vanishes. Therefore, δ'_κ is the only phase that can be freely chosen.

Finally, we present the effects of δ'_κ on the masses and couplings of the Higgs mass eigenstates with $\delta_{\rm EDM} = 0$. For illustration, we consider two parameter sets with $\kappa = -0.2$ and $\kappa = -0.9$, while the other parameters are the same as in Fig. 4, and we plot the δ'_κ dependences of the masses and couplings in Figs. 6 and 7, respectively. In order to allow comparison with previous results, a positive value of R_κ in Eq. (5·1) was chosen. As shown in Figs. 6 and 7, the phase dependences in the light Higgs scenario ($\kappa = -0.2$) are weaker than in the heavy Higgs scenario ($\kappa = -0.9$), because $|\kappa|$ is smaller for the light Higgs scenario. In Fig. 6, the next-to-lightest Higgs boson h_2 becomes lighter than 114 GeV for $\delta'_\kappa/\pi < 0.31$, and hence a large value of δ'_k is not allowed by the spectrum condition. From Fig. 7 it is seen that the model is not feasible for $\delta'_\kappa/\pi > 0.24$, because of the small Higgs mass with moderate gauge

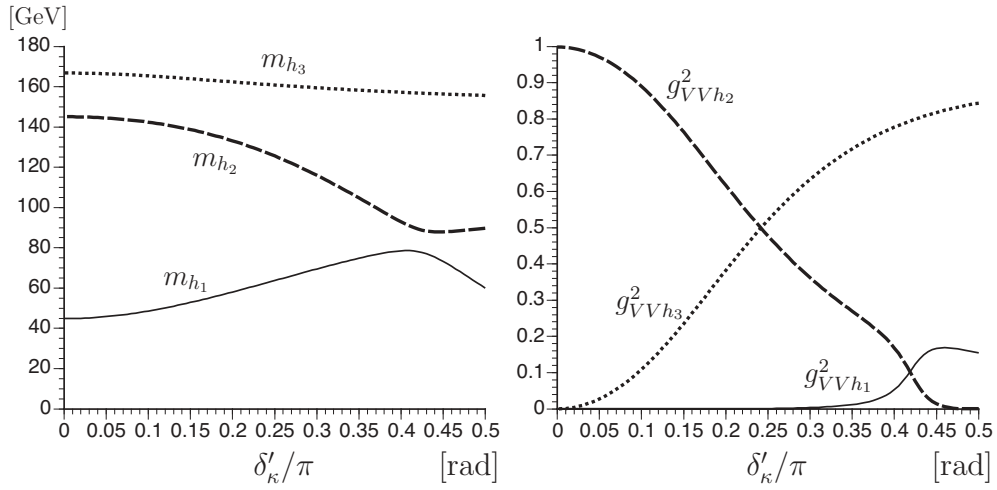

Fig. 6. The Higgs masses and couplings as functions of δ'_κ, with the same parameter values as in Fig. 4, but with $\kappa = -0.2$ (light Higgs scenario) and $\delta_{\rm EDM} = 0$.

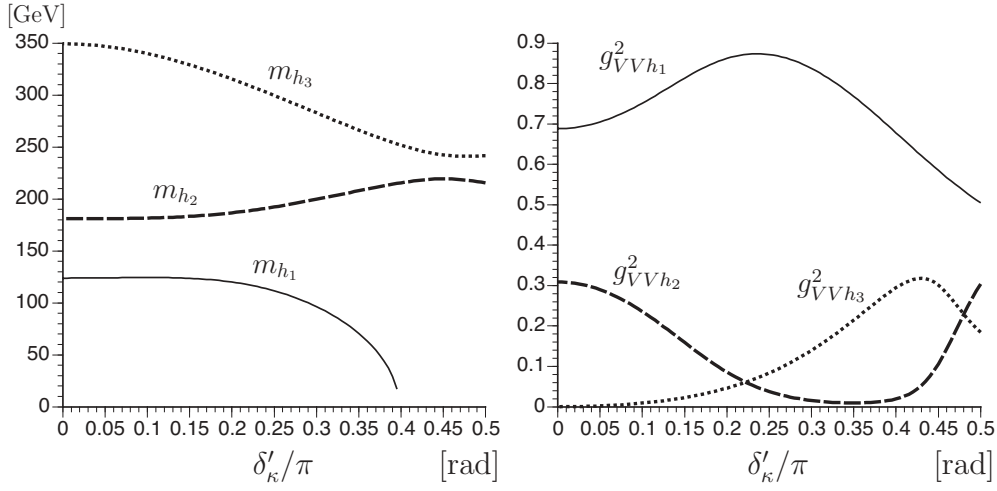

Fig. 7. The same as Fig. 6, but with $\kappa = -0.9$ (heavy Higgs scenario).

coupling, and also for $\delta'_\kappa/\pi > 0.39$, where the prescribed vacuum becomes unstable. We have not found an example in which an excluded parameter set becomes allowed as a light Higgs as a result of the introduction of CP violation in the tree-level Higgs sector. However, a light Higgs boson is realized even for the heavy Higgs parameter sets when we introduce CP violation in the squark sector, in the same way as in the MSSM.

§6. Summary

We have investigated the spectrum and coupling constants of Higgs bosons in the NMSSM in the case that the vacuum expectation value of the singlet is of the weak scale for wide ranges of values of all the parameters in the model. We formulated the mass matrices of the neutral Higgs bosons and the charged Higgs mass independently of the phase convention in CP-violating case. Using of the effective potential including one-loop corrections of the third generation of quarks and squarks, we obtained constraints on the parameters of the model. Then, we required that the neutral Higgs boson whose coupling to the Z boson is not so small be heavier than 114 GeV and that the prescribed vacuum be the absolute minimum of the effective potential. The latter condition is nontrivial in the NMSSM, in contrast to the MSSM, in which the electroweak vacuum is the global minimum of the potential as long as the symmetry breaking conditions are satisfied. We found that the vacuum condition leads to an upper bound on the charged Higgs boson, which is irrelevant in the MSSM limit but effective in our case, in which of $\langle N \rangle = O(100)$ GeV. The allowed parameter regions are classified into two distinct sets: one allows a light scalar with a very small gauge coupling, while the other contains scalars whose masses exceed the bound. The former is realized only in the case of a weak scale $\langle N \rangle$ for $\kappa \simeq 0$. The light Higgs bosons in this light Higgs scenario are not inconsistent with experimental data published to this time: the correction factors to the Yukawa coupling of the light bosons are not so large, and those to the Zhh-coupling are so small that the light bosons have not yet been observed in experiments. Therefore, the lightest scalar among those with large gauge coupling, which is the expected to be observed in future collider experiments, behaves just like the Higgs boson in the SM. The SM-like Higgs boson could be as heavy as 150 GeV. Therefore, this model would be regarded as more feasible than the MSSM if the first observed Higgs boson is heavier than 135 GeV.

Another feature of the Higgs sector in the NMSSM is a possible CP violation at the tree level. We studied explicit CP violation in the Higgs sector, which does not affect the neutron EDM. Such a CP violation is likely to play an important role in the scenario of electroweak baryogenesis. For several sets of allowed parameters in the CP-conserving case, we gradually introduced a CP phase and studied its effects on the masses and couplings of the Higgs bosons. As expected, the effect is larger for parameter sets in the heavy Higgs region, which has a larger $|\kappa|$ than the light Higgs scenario. However, we have not found a case in which a large CP violation causes the lightest Higgs boson to be lighter than the present bound on the SM Higgs, while its gauge coupling is sufficiently small that it would not be produced in lepton colliders. Such a situation has been observed in the MSSM, in which the CP violation in the

squark sector induces a large CP violation in the Higgs sector. If such a large CP violation is common to all the generations of squarks, it should be constrained by neutron EDM experiments. We have found that such a CP violation weakens the first-order EWPT in the MSSM with a light stop.[13] Thus the feasible parameter region for electroweak baryogenesis is very limited in the MSSM. As expected on the basis of naive consideration, if the EWPT in the NMSSM is strongly first order because of the trilinear terms in the Higgs potential, there will be a new possibility for baryogenesis.[12] Because the strong phase transition is not caused by a light stop, it should persist even with CP violation in the Higgs sector. Further, the CP violation is not so strongly constrained by EDM experiments. A study of the EWPT in the NMSSM is now in progress.

Acknowledgements

The authors gratefully thank F. Toyoda, A. Kakuto and S. Otsuki for valuable discussions. This work was supported by a grant from the MEXT, Japan (No. 13135222).

Appendix A
—— *The Field Dependent Masses* ——

In this appendix, we list the field-dependent masses of the third generation quarks and squarks and of the gauge bosons. We retain only the neutral components of the Higgs fields, which appear in the definition of the effective potential (3·1) and are necessary for the neutral Higgs mass-squared matrix. For the charged Higgs mass, we need the expressions including the charged Higgs fields ϕ_d^- and ϕ_u^+, but they are almost the same as those in the MSSM,[13] except for replacement of μ with $\lambda v_n e^{i\varphi}/\sqrt{2}$.

The quark masses are expressed in terms of the Higgs fields and vacuum expectation values as

$$\bar{m}_b^2 = |y_b|^2|\phi_d^0|^2 = \frac{1}{2}|y_b|^2(v_d^2 + 2v_d h_d + h_d^2 + a_d^2), \tag{A·1}$$

$$\bar{m}_t^2 = |y_t|^2|\phi_u^0|^2 = \frac{1}{2}|y_t|^2(v_u^2 + 2v_u h_u + h_u^2 + a_u^2), \tag{A·2}$$

where $\phi_d^0 = (v_d + h_d + ia_d)/\sqrt{2}$ and $\phi_u^0 = e^{i\theta}(v_u + h_u + ia_u)/\sqrt{2}$. If we take the Higgs fields as $h_d = h_u = h_n = 0$, the masses at the vacuum are obtained as

$$\langle \bar{m}_b^2 \rangle = m_b^2 = \frac{1}{2}|y_b|^2 v_d^2, \quad \langle \bar{m}_t^2 \rangle = m_t^2 = \frac{1}{2}|y_t|^2 v_u^2, \tag{A·3}$$

where the brackets indicate the vacuum expectation value. The field dependent masses of the gauge bosons are

$$\bar{m}_Z^2 = \frac{g_2^2 + g_1^2}{2}(|\phi_d^0|^2 + |\phi_u^0|^2), \quad \bar{m}_W^2 = \frac{g_2^2}{2}(|\phi_d^0|^2 + |\phi_u^0|^2). \tag{A·4}$$

Then, the gauge bosons masses are

$$\langle \bar{m}_Z^2 \rangle = m_Z^2 = \frac{g_2^2+g_1^2}{4}(v_d^2+v_u^2), \quad \langle \bar{m}_W^2 \rangle = m_W^2 = \frac{g_2^2}{4}(v_d^2+v_u^2). \tag{A·5}$$

Similarly, the field dependent top- and bottom-squark masses are

$$\bar{m}_{\tilde{t}_{1,2}}^2 = \frac{1}{2}\Bigg[m_{\tilde{q}}^2 + m_{\tilde{t}_R}^2 + \frac{g_2^2+g_1^2}{4}(|\phi_d^0|^2-|\phi_u^0|^2) + 2|y_t|^2|\phi_u^0|^2 \pm \sqrt{(m_{\tilde{q}}^2 - m_{\tilde{t}_R}^2 + x_t(|\phi_d^0|^2-|\phi_u^0|^2))^2 + 4|y_t|^2|\lambda n\phi_d^0 - A_t^*\phi_u^{0*}|^2}\Bigg], \tag{A·6}$$

$$\bar{m}_{\tilde{b}_{1,2}}^2 = \frac{1}{2}\Bigg[m_{\tilde{q}}^2 + m_{\tilde{b}_R}^2 - \frac{g_2^2+g_1^2}{4}(|\phi_d^0|^2-|\phi_u^0|^2) + 2|y_b|^2|\phi_d^0|^2 \pm \sqrt{(m_{\tilde{q}}^2 - m_{\tilde{b}_R}^2 + x_b(|\phi_d^0|^2-|\phi_u^0|^2))^2 + 4|y_b|^2|\lambda n\phi_u^0 - A_b^*\phi_d^{0*}|^2}\Bigg], \tag{A·7}$$

where

$$x_t \equiv \frac{1}{4}\left(g_2^2 - \frac{5}{3}g_1^2\right), \quad x_b \equiv -\frac{1}{4}\left(g_2^2 - \frac{1}{3}g_2^2\right).$$

The masses of the squarks at the vacuum are

$$\left\langle \bar{m}_{\tilde{t}_{1,2}}^2 \right\rangle = m_{\tilde{t}_{1,2}}^2 = \frac{1}{2}\Bigg[m_{\tilde{q}}^2 + m_{\tilde{t}_R}^2 + \frac{g_2^2+g_1^2}{8}(v_d^2-v_u^2) + |y_t|^2 v_u^2 \pm\sqrt{M_t^2 + 2|y_t|^2(P_t v_d^2 + Q_t v_u^2)}\Bigg], \tag{A·8}$$

$$\left\langle \bar{m}_{\tilde{b}_{1,2}}^2 \right\rangle = m_{\tilde{b}_{1,2}}^2 = \frac{1}{2}\Bigg[m_{\tilde{q}}^2 + m_{\tilde{b}_R}^2 - \frac{g_2^2+g_1^2}{8}(v_d^2-v_u^2) + |y_b|^2 v_d^2 \pm\sqrt{M_b^2 + 2|y_b|^2(P_b v_u^2 + Q_b v_d^2)}\Bigg], \tag{A·9}$$

where we have defined the following combinations of the parameters:

$$\begin{aligned}
R_q &= \frac{1}{\sqrt{2}}\mathrm{Re}(\lambda A_q e^{i(\theta+\phi)}), & I_q &= \frac{1}{\sqrt{2}}\mathrm{Im}(\lambda A_q e^{i(\theta+\phi)}), \quad (q=t,b)\\
P_t &= \frac{1}{2}|\lambda|^2 v_n^2 - R_t v_n \tan\beta, & Q_t &= |A_t|^2 - R_t v_n \cot\beta,\\
P_b &= \frac{1}{2}|\lambda|^2 v_n^2 - R_b v_n \cot\beta, & Q_b &= |A_b|^2 - R_b v_n \tan\beta,\\
M_t^2 &= m_{\tilde{q}}^2 - m_{\tilde{t}_R}^2 + \frac{x_t}{2}(v_d^2-v_u^2), & M_b^2 &= m_{\tilde{q}}^2 - m_{\tilde{b}_R}^2 + \frac{x_b}{2}(v_d^2-v_u^2).
\end{aligned} \tag{A·10}$$

Although I_q does not appear in the above equations, we define it here for later convenience. (We use I_q in Appendix B)

Appendix B

—— *Derivatives of the Squark Masses* ——

The corrections to the neutral-mass matrix from the squark loops contain first derivatives of the field-dependent squark masses and the matrices $\mathcal{T}^S$, $\mathcal{T}^P$, $\mathcal{T}^{SP}$, $\mathcal{B}^S$,

$\mathcal{B}^P$ and $\mathcal{B}^{SP}$ (3·11)–(3·17). The first derivatives of the squark masses are as follows:

$$\left\langle \frac{\partial \bar{m}^2_{\tilde{t}_{1,2}}}{\partial \boldsymbol{h}} \right\rangle = \begin{pmatrix} \frac{g_2^2+g_1^2}{8} v_d \\ \left(|y_t|^2 - \frac{g_2^2+g_1^2}{8}\right) v_u \\ 0 \end{pmatrix} \pm \frac{\boldsymbol{t}}{2\Delta m^2_{\tilde{t}}}, \quad \left\langle \frac{\partial \bar{m}^2_{\tilde{t}_{1,2}}}{\partial \boldsymbol{a}} \right\rangle = \pm \frac{|y_t|^2}{\Delta m^2_{\tilde{t}}} I_t v_n \boldsymbol{p}, \tag{B·1}$$

$$\left\langle \frac{\partial \bar{m}^2_{\tilde{b}_{1,2}}}{\partial \boldsymbol{h}} \right\rangle = \begin{pmatrix} \left(|y_b|^2 - \frac{g_2^2+g_1^2}{8}\right) v_d \\ \frac{g_2^2+g_1^2}{8} v_u \\ 0 \end{pmatrix} \pm \frac{\boldsymbol{b}}{2\Delta m^2_{\tilde{b}}}, \quad \left\langle \frac{\partial \bar{m}^2_{\tilde{b}_{1,2}}}{\partial \boldsymbol{a}} \right\rangle = \pm \frac{|y_b|^2}{\Delta m^2_{\tilde{b}}} I_b v_n \boldsymbol{p}, \tag{B·2}$$

where

$$\boldsymbol{t} = \begin{pmatrix} (x_t M_t^2 + 2|y_t|^2 P_t) v_d \\ (-x_t M_t^2 + 2|y_t|^2 Q_t) v_u \\ 2|y_t|^2 P_t \frac{v_d^2}{v_n} \end{pmatrix}, \qquad \boldsymbol{b} = \begin{pmatrix} (x_b M_b^2 + 2|y_b|^2 Q_b) v_d \\ (-x_b M_b^2 + 2|y_b|^2 P_b) v_u \\ 2|y_b|^2 P_b \frac{v_u^2}{v_n} \end{pmatrix},$$

$$\boldsymbol{p} = \frac{1}{v_n} \begin{pmatrix} v_u v_n \\ v_n v_d \\ v_d v_u \end{pmatrix}, \qquad \Delta m^2_{\tilde{q}} = m^2_{\tilde{q}_1} - m^2_{\tilde{q}_2}. \quad (q = t, b) \tag{B·3}$$

The explicit forms of the matrices $\mathcal{T}^S$ and $\mathcal{B}^S$ are

$$\mathcal{T}^S = \begin{pmatrix} \frac{x_t^2}{2} v_d^2 & -\frac{x_t^2}{2} v_d v_u & |y_t \lambda|^2 v_n v_d \\ -\frac{x_t^2}{2} v_d v_u & \frac{x_t^2}{2} v_u^2 & 0 \\ |y_t \lambda|^2 v_n v_d & 0 & 0 \end{pmatrix} + |y_t|^2 R_t \begin{pmatrix} \frac{v_u v_n}{v_d} & -v_n & -v_u \\ -v_n & \frac{v_n v_d}{v_u} & -v_d \\ -v_u & -v_d & \frac{v_d v_u}{v_n} \end{pmatrix} - \frac{\boldsymbol{t}\boldsymbol{t}^T}{2(\Delta m^2_{\tilde{t}})^2}, \tag{B·4}$$

and

$$\mathcal{B}^S = \begin{pmatrix} \frac{x_b^2}{2} v_d^2 & -\frac{x_b^2}{2} v_d v_u & 0 \\ -\frac{x_b^2}{2} v_d v_u & \frac{x_b^2}{2} v_u^2 & |y_b \lambda|^2 v_n v_u \\ 0 & |y_b \lambda|^2 v_n v_u & 0 \end{pmatrix} + |y_b|^2 R_b \begin{pmatrix} \frac{v_u v_n}{v_d} & -v_n & -v_u \\ -v_n & \frac{v_n v_d}{v_u} & -v_d \\ -v_u & -v_d & \frac{v_d v_u}{v_n} \end{pmatrix} - \frac{\boldsymbol{b}\boldsymbol{b}^T}{2(\Delta m^2_{\tilde{b}})^2}. \tag{B·5}$$

These are obtained from the second derivatives of $\Delta_{\tilde{q}} V$ with respect to h_d, h_u and h_n and applying the tadpole conditions. The corrections to the pseudoscalar and scalar-pseudoscalar-mixing components of the neutral-mass matrix include the following matrices:

$$\mathcal{T}^P = \left[|y_t|^2 R_t \frac{v_n}{v_d v_u} - 2 \left(\frac{|y_t|^2 I_t v_n}{\Delta m^2_{\tilde{t}}} \right)^2 \right] \boldsymbol{p}\boldsymbol{p}^T, \quad \mathcal{B}^P = \left[|y_b|^2 R_b \frac{v_n}{v_d v_u} - 2 \left(\frac{|y_b|^2 I_b v_n}{\Delta m^2_{\tilde{b}}} \right)^2 \right] \boldsymbol{p}\boldsymbol{p}^T. \tag{B·6}$$

6 and

$$\mathcal{T}^{SP} = \frac{|y_t|^2 I_t v_n}{(\Delta m_{\tilde{t}}^2)^2} \boldsymbol{t}\boldsymbol{p}^T, \quad \mathcal{B}^{SP} = \frac{|y_b|^2 I_b v_n}{(\Delta m_{\tilde{b}}^2)^2} \boldsymbol{b}\boldsymbol{p}^T. \tag{B·7}$$

References

1) R. Barate et al. (ALEPH Collaboration), Phys. Lett. B **565** (2003), 61; hep-ex/0306033.
2) S. Eidelman et al. (Particle Data Group Collaboration), Phys. Lett. B **592** (2004), 1.
3) Y. Okada, M. Yamaguchi and T. Yanagida, Prog. Theor. Phys. **85** (1991), 1.
J. R. Ellis, G. Ridolfi and F. Zwirner, Phys. Lett. B **257** (1991), 83.
J. R. Espinosa and R.-J. Zhang, Nucl. Phys. B **586** (2000), 3; hep-ph/0003246.
4) P. Fayet, Nucl. Phys. B **90** (1975), 104.
5) J. F. Gunion and H. E. Haber, Nucl. Phys. B **272** (1986), 1.
6) J. R. Ellis, J. F. Gunion, H. E. Haber, L. Roszkowski and F. Zwirner, Phys. Rev. D **39** (1989), 844.
7) D. J. Miller, R. Nevzorov and P. M. Zerwas, Nucl. Phys. B **681** (2004), 3; hep-ph/0304049.
8) A. Pilaftsis and C. E. M. Wagner, Nucl. Phys. B **553** (1999), 3; hep-ph/9902371.
M. Carena, J. R. Ellis, A. Pilaftsis and C. E. M. Wagner, Nucl. Phys. B **586** (2000), 92; hep-ph/0003180.
9) The OPAL Collaboration, Physics Note PN524.
10) U. Ellwanger, M. Rausch de Traubenberg and C. A. Savoy, Nucl. Phys. B **492** (1997), 21; hep-ph/9611251.
G. C. Branco, F. Kruger, J. C. Romao and A. M. Teixeira, J. High Energy. Phys. **07** (2001), 027; hep-ph/0012318.
A. T. Davies, C. D. Froggatt and A. Usai, Phys. Lett. B **517** (2001), 375.
11) M. Matsuda and M. Tanimoto, Phys. Rev. D **52** (1995), 3100; hep-ph/9504260.
N. Haba, Prog. Theor. Phys. **97** (1997), 301; hep-ph/9608357.
S. W. Ham, J. Kim, S. K. Oh and D. Son, Phys. Rev. D **64** (2001), 035007; hep-ph/0104144.
S. W. Ham, S. K. Oh and D. Son, Phys. Rev. D **65** (2002), 075004.
12) M. Dine, P. Huet and J. R. Singleton, Nucl. Phys. B **375** (1992), 625.
M. Pietroni, Nucl. Phys. B **402** (1993), 27; hep-ph/9207227.
A. T. Davies, C. D. Froggatt and R. G. Moorhouse, Phys. Lett. B **372** (1996), 88; hep-ph/9603388.
S. J. Huber and M. G. Schmidt, Eur. Phys. J. C **10** (1999), 473; hep-ph/9809506; Nucl. Phys. B **606** (2001), 183; hep-ph/0003122.
M. G. Schmidt, Nucl. Phys. Proc. Suppl. **101** (2001), 39; hep-ph/0102043.
13) K. Funakubo, S. Tao and F. Toyoda, Prog. Theor. Phys. **109** (2003), 415; hep-ph/0211238.
14) B. A. Dobrescu and K. T. Matchev, J. High Energy. Phys. **09** (2000), 031; hep-ph/0008192.
15) S. A. Abel, S. Sarkar and P. L. White, Nucl. Phys. B **454** (1995), 663; hep-ph/9506359.
16) A. Menon, D. E. Morrissey and C. E. M. Wagner, Phys. Rev. D **70** (2004), 035005; hep-ph/0404184.
17) L. Babukhadia et al. (CDF and D0 Working Group Members Collaboration), FERMILAB-PUB-03-320-E.
D. Denegri, V. Drollinger, R. Kinnunen, K. Lassila-Perini, S. Lehti, F. Moortgat, A. Nikitenko, S. Slabospitsky and N. Stepanov, CMS-NOTE-2001-032; hep-ph/0112045.
18) S. Gentile, ATL-PHYS-2004-009.
S. Asai et al., Eur. Phys. J. C **32** S2 (2004), 19; hep-ph/0402254.
K. A. Assamagan and Y. Coadou, Acta Phys. Polon. B **33** (2002), 1347.
19) G. Abbiendi et al. (OPAL Collaboration), Eur. Phys. J. C **18** (2001), 425; hep-ex/0007040.
20) G. Abbiendi et al. (OPAL Collaboration), Eur. Phys. J. C **23** (2002), 397; hep-ex/0111010.
21) V. M. Abazov et al. (D0 Collaboration), Phys. Rev. Lett. **94** (2005), 091802; hep-ex/0410062.